Viscosity and density measurements of aqueous amines at high pressures: MDEA-water and MEA-water mixtures for CO_2 capture

Manuel Sobrino, Eduardo I. Concepción, Ángel Gómez-Hernández, M. Carmen Martín, José J. Segovia*

TERMOCAL Research Group, Escuela de Ingenierías Industriales, Universidad de Valladolid, Paseo del Cauce 59, 47011 Valladolid, Spain.

*corresponding autor, e-mail: jose.segovia@eii.uva.es

ABSTRACT

Viscosity and density are thermophysical properties crucial to characterizing any kind of fluid such as aqueous amines. These blends are becoming more and more relevant for their CO_2 capture potential, such that having accurate viscosity and density measurements would prove useful. Densities and viscosities of these mixtures at atmospheric pressure may be found in the literature although it is more difficult to find values at high pressures, these potentially proving interesting when seeking to provide a full description of these fluids.

Viscosity and density measurements at high pressures (up to 120 MPa) and at temperatures between 293.15 and 353.15 K of MDEA + water and MEA + water mixtures (both from 10 % to 40 % amine mass fraction) are presented in this work. Density measurements were performed with an Anton Paar DMA HPM densimeter with an expanded uncertainty (k = 2) less than ± 0.7 $kg \cdot m^{-3}$. A falling body technique was used to measure viscosities at high pressures due to its sturdiness in terms of corrosion. Details of this latter equipment are presented, including calibration using *n*-dodecane and uncertainty calculations, which give a relative expanded uncertainty (k = 2) of less than ± 2.4 % for the highest viscosity and ± 2.9 % for the lowest.

Keywords: Viscosity; Density; Falling body viscometer; High pressure; MDEA; MEA.

1. Introduction

Society is becoming increasingly aware of environmental issues, with the focus on problems such as the greenhouse effect. In this sense, reducing CO_2 emissions is an important goal. Although there are many substances whose Global Warming Potential (GWP) is higher than the GWP of CO_2, our current way of life, which is mainly based on fossil fuels, forces us to pay particular attention to CO_2 emissions.

There are two main actions which might help to improve this situation. Firstly, an increased use of renewable sources will reduce CO_2 emissions directly, and secondly, CO_2 may be removed from gas streams by using substances such as aqueous amines. In this regard, many initiatives have been promoted by governments over the last few years in an effort to cut CO_2 emissions.

Specifically, alkanolamine solutions are widely used in industry to remove components such as H_2S and CO_2 from natural or refinery gases, with the tertiary amine *n*-methyldiethanolamine (MDEA) an industrially important one for this purpose [1, 2]. Primary amine monoethanolamine (MEA) is one of the most effective amines for CO_2 absorption, reaching efficiency rates above 90 % [3] and being catalogued as one of the most promising amines for these purposes by Aaron et al. [4].

Thermophysical properties such as viscosity and density of aqueous solutions are required for two main reasons. Firstly, they are crucial for designing treatment equipment [5], and secondly, knowledge of these properties, even at high pressures, will enable a full characterization of these fluids.

In this work, viscosity and density measurements of MDEA + H_2O and MEA + H_2O mixtures (10 %, 20 %, 30 % and 40 % amine mass fraction) at pressures from 0.1 to 120 MPa and

temperatures of 293.15, 313.15, 333.15 and 353.15 K are presented. Density measurements were carried out with an Anton Paar DMA HPM densimeter, already introduced [6], and density measurements were extended up to p = 140 MPa and T = 393.15 K. Viscosity measurements were performed with a falling body viscometer recently developed at the TERMOCAL laboratory [7]. Both techniques are able to resist any corrosion effects which might be caused by amines.

2. Experimental procedure

2.1. Densimeter

An Anton Paar DMA HPM densimeter was employed to perform the density measurements using water and vacuum for its calibration and following the method shown in [6]. Uncertainty calculations were carried out following the procedure described in JCGM 100:2008 [8] and explained in [6], obtaining an expanded uncertainty (k = 2) of below ± 0.7 $kg \cdot m^{-3}$.

2.2 Viscometer

A falling body viscometer was used for the measurements. It is based on the falling time measurement of a body (a cylinder in our case) when it falls through a vertical pipe containing the fluid whose viscosity we wish to know. The apparatus is able to measure in wide pressure ranges, from 0.1 MPa to 140 MPa, and temperature, from 253.15 K to 523.15 K.

The cell, where measurements take place, was designed by the Groupe de Haute Pression, Laboratoire des Fluides Complexes of the University of Pau [9], and its full experimental setup was developed and improved at the TERMOCAL laboratory.

Considering that the body reaches its terminal velocity without eccentricity and laminar flow, equation (1) could theoretically describe the behaviour of this sort of viscometers. This expression is based on the Stokes' law and Newton's second law:

$$\eta = K \cdot \Delta\rho \cdot \Delta t \quad (1)$$

The terms of the expression (1) are: η the viscosity, K a calibration constant which depends on the apparatus and the falling body, $\Delta\rho$ the difference between the density of the body material and the liquid density, and Δt the time registered between two coils.

In an ideal case, K could be determined without any calibration from the dimensions of the instrument, the mass of the falling cylinder and its density using a mathematical expression. However, in practice, this is not advisable because real operation of this instrument differs from the simplified model given by that mathematical expression in several factors [10,11], which is why a calibration procedure is always performed in this kind of viscometer. Several ways of calibration based on equation (1) have been successfully performed [12]: from the use of a single calibration constant modified by thermal expansion coefficients to using several calibration constants for each temperature and pressure set.

In our case, the model described by equation (1) fits the range of viscosities considering in this work (up to 5 mPa·s approximately) quite well. However, adding an independent term (intercept) to the expression (1) has allowed us to achieve a better approach to the behaviour of our viscometer. Expression (2) is therefore used in this work:

$$\eta = a + b \cdot \Delta t \cdot \Delta\rho \quad (2)$$

Although this expression has already been used by other authors, it is important to highlight how it is used. As will be shown in the calibration procedure, equation (2) would be applied regardless temperature and pressure. This offers a substantial advantage since we can measure at any temperature and pressure condition with a single fitting, as long as measured viscosities are within its calibration range.

The experimental setup was developed in full at the TERMOCAL laboratory using high pressure equipment and was described in [13]. The principal elements are the measuring cell, a rotary valve which allows us to rotate the cell automatically, a thermostatic bath (Julabo

F81-ME), a pressure generator (HiP 50-5.75-30), a digital gauge (Druck DPI 104), a vacuum pump (Leybold TRIVAC D8B) with a cold trap, and the electronic devices: 16 Ch. Multifunction Data Acquisition Unit 16 bits (Agilent U2352A), Data Acquisition Unit for the temperature (Agilent 34970A), Arbitrary Waveform Generator (Agilent, 33220A). In addition, resistance thermometers attached to the coils were installed to control temperature and another pressure generator (HiP 50-6-15) linked to an engine was added to control the pressure automatically.

The measuring cell, which is the core of this viscometer, is presented in Figure 1. It has two concentric tubes whose length is 400 mm and their diameters are 6.52 mm and 8.1 mm. Both of them are filled with the pressurized liquid, maintaining the same pressure inside and outside the inner tube and avoiding any risk of deformation. In addition, four coils, spaced 50 mm apart, are arranged around the tube. Those coils are placed towards the bottom so as to favour terminal velocity being reached. It has been proved in a previous work [14] that terminal velocity is reached in all the cases. Thus, in order to avoid signal interferences between coils, the two intermediate coils are disconnected, and the time from the first to the fourth coil (separated by 150 mm) is taken. Tubes and coils are surrounded by a thermostatic fluid which flows from the bath. The falling cylinder (shown in Figure 1) is made of magnetic stainless steel with a hemispherical end and has a length of 20 mm and a diameter of 6.20 mm. The density of the body (approximately constant) is determined using a pycnometer ρ = (7.673 ± 0.017) g·cm^{-3}. The relationship between the diameter of the inner tube and the diameter of the falling body is 0.951. This value is higher than the critical value of 0.93 established by Chen et al. [15] and also higher than the more conservative value of 0.95 established by Vant and used by Schaschke et al. [16] and Zeng et al. [11]. Working below those values could cause undesirable eccentricity effects.

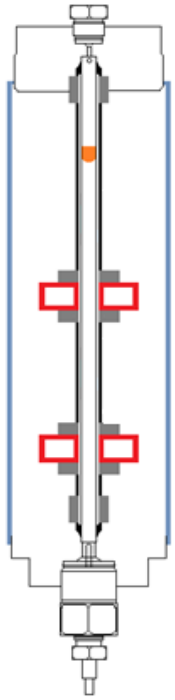

Figure 1. Measuring cell with two operating coils.

A time measurement system was designed and described previously [7,17] and allows time to be measured with an expanded uncertainty ($k = 2$) of ± 0.01 s.

A computer program using Agilent VEE Pro software was developed in full at the TERMOCAL laboratory to record all the parameters involved in our measurements (falling time, pressure, temperature…). This time measurement system is an important improvement for such falling body techniques and provide accurate time measurements which implies accurate viscosities.

2.3 Materials

The materials used in the calibration and the measurements were used without further purification and their purity was checked by gas chromatography. Table 1 summarizes their characteristics.

Table 1. Material description.

Compound	Source	Mass fraction purity[a]	Water content (%)	Purification method
n-Dodecane	Sigma-Aldrich	≥ 0.99	Máx. 0.01	None
1-Butanol	Sigma-Aldrich	≥ 0.995	Máx. 0.1 (157.5 ppm)	None
MDEA	Aldrich Chemistry	≥ 0.999	Máx. 0.1	None
MEA	Sigma-Aldrich	≥ 0.998	Máx. 0.14	None
Water	Sigma-Aldrich	Conductivity ≤ $2 \cdot 10^{-6}$ $ohm^{-1} \cdot cm^{-1}$		None

[a] As stated by the supplier and checked by gas chromatography.

2.4 Viscometer calibration

Calibration of the falling body viscometer was performed from 0.1 MPa to 120 MPa and from 293.15 K to 353.15 K with *n*-dodecane as calibration fluid and the correlation proposed by Caudwell et al. [18] was used. It is important to highlight that Caudwell et al. [18] correlation begins at 298.15 K, so data for calibration at 293.15 K were also taken from [13], both data based on vibrating wire viscometer measurements.

Fall time was recorded considering fifteen repetitions for each pressure and temperature. After that, calibration consists of fitting all points (figure 2) using the model expressed by equation (2), whose R-squared value indicates that the model defined by the parameters given in table 2 explains 99.89 % of variability.

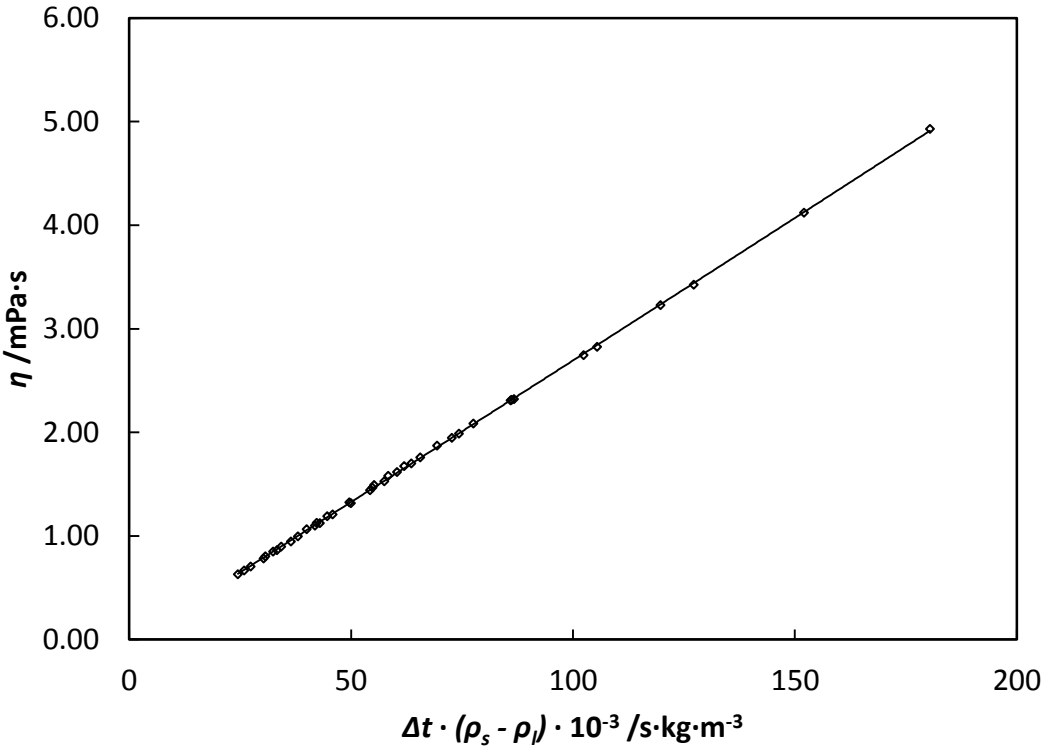

Figure 2. Falling body viscometer calibration fitting using *n*-dodecane as reference fluid.

Table 2. Coefficients of equation (2) obtained for the falling body viscometer calibration with *n*-dodecane.

	Parameters	**Standard deviation**
a / mPa·s	$-4.49383 \cdot 10^{-2}$	$8.7 \cdot 10^{-3}$
b / mPa·m^3·kg^{-1}	$2.77769 \cdot 10^{-5}$	$1.1 \cdot 10^{-7}$

According to the procedure described, the range of the present calibration is from η = 0.630 mPa·s (*n*-dodecane at T = 353.15 K and p = 0.1 MPa) to η = 4.929 mPa·s (*n*-dodecane at T = 293.15 K and p = 120 MPa).

2.5. Uncertainty calculation for viscosity

Uncertainty calculation was carried out following the model expressed by equation (2) and the procedure described in JCGM 100:2008 [8] and its results are presented in tables 3 and 4 [17]. Uncertainty was evaluated at the limits of the calibration viscosity range for the studied mixtures, whose results are presented in the next section: the lowest viscosity (0.617 mPa·s, MDEA 20 % + H_2O at T = 353.15 K and p = 0.1 MPa) and the highest viscosity (4.954 mPa·s, MEA 40 % + H_2O at T = 293.15 K and p = 120 MPa). It has been considered a normal distribution with a coverage factor k = 2 (confidence level of 95.45 %), obtaining a relative expanded uncertainty which varies from ± 2.4 % to ± 2.9 % for the highest and lowest viscosities, respectively. It is interesting to highlight that the most significant contribution in both cases is the uncertainty associated to calibration function coefficients.

Table 3. Uncertainty calculation of dynamic viscosity, η, for MEA (1)+ H_2O (2) (w_1 = 0.4001) at p = 120 MPa and T = 293.15 K.

Amount		Estimate	Units	Probability Distribution	Standard Uncertainty	Coefficient of Sensitivity	Contribution to Uncertainty
X_i		x_i			$u(x_i)$	c_i	$u(y)$
Reference Fluid	Viscosity	4.954	mPa·s	Normal	0.050	1	0.050
Time	Calibration		s	Normal	0.005	0.19	0.0010
	Resolution	27.20	s	Rectangular	0.0029	0.19	0.00056
	Repeatability		s	Normal	0.070	0.19	0.014
Temperature	Calibration		K	Normal	0.010	0.085	0.00085
	Resolution	293.15	K	Rectangular	0.0029	0.085	0.00025
	Uniformity		K	Rectangular	0.029	0.085	0.0025
	Stability		K	Rectangular	0.014	0.085	0.0012
Pressure	Calibration		MPa	Normal	0.00001	0.040	0.0000
	Resolution	120	MPa	Rectangular	0.0029	0.040	0.00012
	Stability		MPa	Rectangular	0.014	0.040	0.00058
Density	Solid	7673	$kg \cdot m^{-3}$	Normal	17	0.00073	0.012
	Fluid	1056.3	$kg \cdot m^{-3}$	Normal	0.42	0.00073	0.00031
Calibration function coefficients			mPa·s	Normal	0.030	1	0.030
Standard Uncertainty			mPa·s			$u(y)$	± 0.061
Expanded Uncertainty (k=2)			mPa·s			$U(y)$	± 0.12
Relative Expanded Uncertainty (k=2)			(mPa·s/mPa·s)			$U_r(y)$	± **0.024**

Table 4. Uncertainty calculation of dynamic viscosity, η, for MDEA (1) + H_2O (2) (w_1 = 0.2002) at p = 0.1 MPa and T = 353.15 K.

Amount		Estimate	Units	Probability Distribution	Standard Uncertainty	Coefficient of Sensitivity	Contribution to Uncertainty
X_i		x_i			$u(x_i)$	c_i	$u(y)$
Reference Fluid	Viscosity	0.617	mPa·s	Normal	0.0062	1	0.0062
Time	Calibration		s	Normal	0.005	0.18	0.0009
	Resolution	3.56	s	Rectangular	0.0029	0.18	0.00052
	Repeatability		s	Normal	0.009	0.18	0.0016
Temperature	Calibration		K	Normal	0.010	0.0087	0.000087
	Resolution	353.15	K	Rectangular	0.0029	0.0087	0.000025
	Uniformity		K	Rectangular	0.029	0.0087	0.00025
	Stability		K	Rectangular	0.014	0.0087	0.00013
Pressure	Calibration		MPa	Normal	0.00001	0.0075	0.000000
	Resolution	0.1	MPa	Rectangular	0.0029	0.0075	0.000022
	Stability		MPa	Rectangular	0.014	0.0075	0.00011
Density	Solid	7673	$kg \cdot m^{-3}$	Normal	17	0.00010	0.0017
	Fluid	985.3	$kg \cdot m^{-3}$	Normal	0.39	0.00010	0.00004
Calibration function coefficients			mPa·s	Normal	0.0059	1	0.0059
Standard Uncertainty		mPa·s				$u(y)$	±± 0.0089
Expanded Uncertainty (k=2)		mPa·s				$U(y)$	± 0.18
Relative Expanded Uncertainty (k=2)		(mPa·s/mPa·s)				$U_r(y)$	± **0.029**

4. Results and discussion

Density measurements of aqueous solutions of methyldiethanolamine (MDEA) and monoethanolamina (MEA) were performed at pressures from 0.1 to 140 MPa for MDEA and up to 120 MPa for MEA and six temperatures from 293.15 to 393.15 K for different amine mass fractions: 0.1, 0.2, 0.3 and 0.4. These experimental results are summarized in table 5 for MDEA and table 6 for MEA.

Table 5. Experimental densities, ρ, for MDEA (1) + H_2O (2) mixtures at different conditions of temperature, T, pressure, p, and mass fraction, w_1.[a]

	ρ/kg·m^{-3}					
	T/K					
p/MPa	293.15	313.15	333.15	353.15	373.15	393.15
	w_1 = 0.1000					
0.1	1007.0	1000.2	990.5	978.6	964.4	948.6
0.5	1007.2	1000.4	990.6	978.7	964.6	949.0
1	1007.4	1000.6	990.8	978.9	964.9	949.2
2	1007.8	1001.0	991.3	979.3	965.3	949.6
5	1009.0	1002.2	992.5	980.6	966.7	951.1
10	1011.1	1004.3	994.6	982.8	969.0	953.6
15	1013.2	1006.3	996.6	984.9	971.2	956.0
20	1015.3	1008.2	998.6	987.0	973.5	958.5
30	1019.4	1012.3	1002.6	991.2	977.9	963.0
40	1023.4	1016.2	1006.7	995.2	982.1	967.6
50	1027.3	1019.9	1010.4	999.1	986.2	971.8
60	1031.1	1023.8	1014.2	1003.1	990.1	976.2
70	1035.0	1027.4	1017.9	1006.9	994.2	980.4
80	1038.5	1031.0	1021.6	1010.5	998.1	984.3

90	1042.2	1034.5	1025.1	1014.0	1001.8	988.3
100	1045.7	1038.2	1028.5	1017.7	1005.3	992.1
110	1049.2	1041.5	1031.9	1021.2	1009.0	995.9
120	1052.7	1044.9	1035.4	1024.6	1012.6	999.6
130	1056.1	1048.1	1038.7	1028.0	1016.0	1003.1
140	1059.5	1051.4	1042.0	1031.2	1019.4	1006.7
			$w_1 = 0.2002$			
0.1	1016.5	1008.5	997.8	985.3	970.5	954.0
0.5	1016.6	1008.6	998.0	985.3	970.7	954.4
1	1016.8	1008.8	998.2	985.5	970.9	954.6
2	1017.2	1009.2	998.6	985.9	971.4	955.2
5	1018.4	1010.4	999.8	987.2	972.8	956.7
10	1020.3	1012.3	1001.8	989.4	975.0	959.2
15	1022.2	1014.2	1003.8	991.5	977.2	961.6
20	1024.2	1016.1	1005.7	993.5	979.5	964.0
30	1028.0	1019.9	1009.7	997.6	983.9	968.5
40	1031.8	1023.7	1013.6	1001.6	988.2	973.1
50	1035.4	1027.3	1017.2	1005.5	992.1	977.3
60	1039.0	1031.0	1020.9	1009.3	996.1	981.7
70	1042.6	1034.4	1024.4	1012.9	1000.0	985.9
80	1045.9	1037.9	1027.9	1016.6	1003.8	989.8
90	1049.4	1041.2	1031.3	1020.0	1007.4	993.7
100	1052.8	1044.7	1034.7	1023.6	1011.1	997.5
110	1056.0	1047.9	1038.0	1027.0	1014.7	1001.4
120	1059.3	1051.1	1041.4	1030.4	1018.3	1005.0
130	1062.6	1054.3	1044.5	1033.6	1021.5	1008.5
140	1065.6	1057.4	1047.7	1036.8	1025.0	1012.0
			$w_1 = 0.3000$			

0.1	1026.7	1017.2	1005.4	992.0	976.5	959.6
0.5	1026.9	1017.4	1005.6	992.0	976.6	959.9
1	1027.1	1017.5	1005.7	992.2	976.9	960.1
2	1027.4	1017.9	1006.2	992.7	977.4	960.6
5	1028.6	1019.1	1007.3	993.9	978.7	962.1
10	1030.4	1020.9	1009.3	996.1	981.1	964.7
15	1032.2	1022.8	1011.3	998.2	983.4	967.1
20	1034.1	1024.6	1013.2	1000.3	985.6	969.6
30	1037.7	1028.4	1017.0	1004.3	989.8	974.2
40	1041.2	1032.0	1020.9	1008.1	994.1	978.7
50	1044.6	1035.5	1024.3	1012.0	998.1	983.0
60	1048.0	1039.0	1027.9	1015.9	1002.1	987.4
70	1051.4	1042.3	1031.5	1019.5	1005.9	991.6
80	1054.6	1045.5	1034.9	1023.0	1009.8	995.4
90	1057.9	1048.7	1038.1	1026.4	1013.3	999.4
100	1061.1	1052.0	1041.6	1029.9	1017.0	1003.1
110	1064.1	1055.2	1044.6	1033.3	1020.5	1006.9
120	1067.2	1058.3	1047.9	1036.6	1024.0	1010.6
130	1070.3	1061.3	1051.0	1039.8	1027.4	1014.1
140	1073.2	1064.5	1054.2	1042.9	1030.7	1017.6
			$w_1 = 0.4000$			
0.1	1036.6	1025.5	1012.4	998.1	981.9	964.2
0.5	1036.8	1025.6	1012.7	998.2	982.1	964.7
1	1036.9	1025.8	1012.8	998.4	982.4	964.8
2	1037.3	1026.2	1013.2	998.8	982.8	965.4
5	1038.3	1027.3	1014.4	1000.1	984.2	966.9
10	1040.1	1029.2	1016.4	1002.3	986.5	969.5

15	1041.9	1031.0	1018.4	1004.4	988.8	972.0
20	1043.6	1032.8	1020.3	1006.5	991.1	974.5
30	1047.1	1036.3	1024.1	1010.5	995.5	979.2
40	1050.4	1040.0	1027.9	1014.4	999.8	983.9
50	1053.8	1043.2	1031.4	1018.2	1003.7	988.1
60	1057.1	1046.6	1035.0	1022.0	1007.7	992.5
70	1060.3	1050.0	1038.4	1025.6	1011.6	996.8
80	1063.3	1053.1	1041.6	1029.1	1015.4	1000.8
90	1066.4	1056.2	1044.9	1032.6	1019.0	1004.6
100	1069.5	1059.5	1048.2	1036.0	1022.6	1008.5
110	1072.4	1062.5	1051.3	1039.3	1026.2	1012.3
120	1075.4	1065.5	1054.5	1042.5	1029.7	1015.9
130	1078.4	1068.4	1057.5	1045.8	1033.0	1019.4
140	1081.1	1071.4	1060.6	1048.9	1036.3	1023.0

[a] Standard uncertainties u are: $u(T)$ = 0.01 K; $u_r(p)$ = 0.0001 (kPa/kPa); $u(w)$ = 0.0001 and $u(\rho)$ = 0.35 kg·m^{-3}

Table 6. Experimental densities, ρ, for MEA (1) + H_2O (2) mixtures at different conditions of temperature, T, pressure, p, and mass fraction, w_1.[a]

	ρ/kg·m^{-3}					
	T/K					
p/MPa	293.15	313.15	333.15	353.15	373.15	393.15
	w_1 = 0.1001					
0.1	1002.5	995.9	986.3	974.7	960.8	945.2
0.5	1002.7	996.0	986.5	974.7	961.0	945.6
1	1002.9	996.3	986.7	975.0	961.3	945.8
2	1003.3	996.6	987.1	975.4	961.8	946.3
5	1004.6	997.9	988.4	976.7	963.1	947.8

10	1006.7	1000.0	990.5	978.9	965.5	950.3
15	1008.8	1002.0	992.6	981.1	967.7	952.7
20	1010.9	1004.0	994.6	983.2	969.9	955.2
30	1015.1	1008.1	998.6	987.4	974.4	959.8
40	1019.1	1012.1	1002.7	991.4	978.7	964.4
50	1023.0	1015.9	1006.5	995.4	982.8	968.7
60	1026.9	1019.8	1010.4	999.4	986.8	973.0
70	1030.8	1023.4	1014.1	1003.1	990.8	977.3
80	1034.5	1027.0	1017.7	1006.9	994.8	981.3
90	1038.2	1030.6	1021.3	1010.5	998.5	985.2
100	1041.8	1034.2	1024.8	1014.1	1002.2	989.1
110	1045.2	1037.6	1028.1	1017.7	1005.9	993.0
120	1048.8	1041.1	1031.7	1021.2	1009.6	996.7
			$w_1 = 0.2000$			
0.1	1006.9	999.1	988.8	976.7	962.5	946.5
0.5	1007.0	999.2	988.9	976.7	962.7	946.9
1	1007.2	999.4	989.1	976.9	962.9	947.0
2	1007.6	999.8	989.5	977.4	963.4	947.5
5	1008.7	1001.0	990.7	978.6	964.7	949.0
10	1010.7	1002.9	992.7	980.8	966.9	951.5
15	1012.6	1004.8	994.7	982.9	969.1	953.8
20	1014.5	1006.7	996.6	984.9	971.3	956.2
30	1018.4	1010.5	1000.5	988.9	975.6	960.7
40	1022.1	1014.3	1004.5	992.9	979.8	965.2
50	1025.8	1017.9	1008.0	996.7	983.7	969.4
60	1029.4	1021.5	1011.7	1000.6	987.7	973.6
70	1033.0	1025.0	1015.2	1004.2	991.5	977.8

80	1036.2	1028.5	1018.7	1007.7	995.4	981.6
90	1039.7	1031.8	1022.1	1011.3	999.0	985.6
100	1043.2	1035.1	1025.5	1014.7	1002.5	989.4
110	1046.4	1038.4	1028.8	1018.2	1006.1	993.0
120	1049.6	1041.8	1032.2	1021.6	1009.6	996.7
			$w_1 = 0.3005$			
0.1	1012.3	1003.2	992.0	979.2	964.5	948.4
0.5	1012.5	1003.4	992.3	979.4	964.8	948.8
1	1012.7	1003.6	992.4	979.6	965.0	948.9
2	1013.0	1004.0	992.8	980.0	965.5	949.4
5	1014.1	1005.1	994.0	981.2	966.8	950.9
10	1016.0	1007.0	996.0	983.3	969.0	953.3
15	1017.7	1008.8	997.9	985.4	971.2	955.7
20	1019.6	1010.6	999.7	987.4	973.4	958.1
30	1023.2	1014.3	1003.5	991.4	977.6	962.6
40	1026.6	1017.9	1007.3	995.2	981.7	967.0
50	1030.0	1021.3	1010.8	999.0	985.6	971.1
60	1033.5	1024.8	1014.4	1002.7	989.5	975.3
70	1036.9	1028.2	1017.8	1006.2	993.3	979.5
80	1040.0	1031.4	1021.1	1009.8	997.1	983.2
90	1043.3	1034.5	1024.4	1013.1	1000.8	987.1
100	1046.6	1037.9	1027.7	1016.6	1004.2	990.9
110	1049.6	1041.0	1031.0	1020.0	1007.7	994.6
120	1052.6	1044.1	1034.2	1023.3	1011.1	998.2
			$w_1 = 0.4000$			
0.1	1018.1	1007.5	995.3	981.9	966.6	950.0
0.5	1018.1	1007.7	995.6	982.0	966.9	950.4
1	1018.3	1007.9	995.8	982.2	967.1	950.6

2	1018.6	1008.3	996.2	982.6	967.6	951.1
5	1019.6	1009.3	997.3	983.9	968.9	952.5
10	1021.4	1011.2	999.3	986.0	971.1	955.0
15	1023.1	1012.9	1001.1	988.0	973.3	957.3
20	1024.8	1014.7	1003.0	990.0	975.4	959.7
30	1028.3	1018.2	1006.7	993.9	979.7	964.3
40	1031.6	1021.7	1010.4	997.7	983.8	968.7
50	1034.8	1025.1	1013.8	1001.4	987.6	972.8
60	1038.1	1028.4	1017.3	1005.1	991.6	977.0
70	1041.4	1031.7	1020.7	1008.6	995.2	981.1
80	1044.3	1034.8	1024.0	1012.1	999.1	985.0
90	1047.5	1037.8	1027.1	1015.3	1002.5	988.8
100	1050.4	1041.1	1030.3	1018.7	1006.0	992.5
110	1053.3	1044.0	1033.5	1022.1	1009.5	996.2
120	1056.3	1047.0	1036.7	1025.2	1012.9	999.7

[a] Standard uncertainties u are: $u(T)$ = 0.01 K; $u_r(p)$ = 0.0001 (kPa/kPa); $u(w)$ = 0.0001 and $u(\rho)$ = 0.35 kg·m^{-3}

Density measurements show that densities of aqueous solutions of MDEA are always higher than the densities of aqueous solutions of MEA for the same conditions of temperature, pressure and composition. The density of these mixtures increases when the weight fraction of the amine is higher and this effect is greater for the solutions with MDEA. Thus, the density differences between MDEA and MEA solutions are higher when the weight fraction of the amine increases. As is expected, density increases when pressure increases or temperature decreases, and these effects are similar for both amine solutions.

The experimental values were correlated using a modified Tammann-Tait equation (equation (3)) for each composition:

$$\rho(T,p) = \frac{A_0 + A_1 T + A_2 T^2}{1 - C \ln\left(\frac{B_0 + B_1 T + B_2 T^2 + p}{B_0 + B_1 T + B_2 T^2 + 0.1MPa}\right)} \quad (3)$$

These results are given in table 7 which contains the fitting parameters and the standard deviation. As can be seen, the experimental results correlate quite well using this equation (3). Although better results are obtained for the mixtures with MDEA, standard deviations are lower than density uncertainties for both amines.

Table 7. Fitting parameters of equation (3) and standard deviations σ for the density measurements

MDEA (1) + H_2O (2)	w_1 = 0.1	w_1 = 0.2	w_1 = 0.3	w_1 = 0.4
A_0/kg·m^{-3}	854.7268	897.2473	955.0871	1017.113
A_1/kg·m^{-3}·K^{-1}	1.35021	1.17809	0.92985	0.65632
A_2/kg·m^{-3}·K^{-2}	-0.002830	-0.002630	-0.002337	-0.002012
B_0/MPa	-675.7028	-128.6144	36.29279	631.3078
B_1/MPa·K^{-1}	6.82909	3.15987	2.14289	-0.49223
B_2/MPa·K^{-2}	-0.011016	-0.005719	-0.004442	-0.5996
C	0.157010	0.121019	0.104427	0.108548
σ/kg·m^{-3}	0.029	0.018	0.0046	0.026
MEA (1) + H_2O (2)	w_1 = 0.1	w_1 = 0.2	w_1 = 0.3	w_1 = 0.4
A_0/kg·m^{-3}	850.8313	893.1019	948.8575	998.3203
A_1/kg·m^{-3}·K^{-1}	1.33316	1.12950	0.85601	0.62575
A_2/kg·m^{-3}·K^{-2}	-0.002781	-0.002528	-0.002181	-0.001904
B_0/MPa	-558.9608	-258.7132	73.8801	323.1854
B_1/MPa·K^{-1}	5.50608	3.96741	2.15210	0.78340
B_2/MPa·K^{-2}	-0.008807	-0.006845	-0.004437	-0.002664
C	0.130217	0.126603	0.120879	0.108548
σ/kg·m^{-3}	0.171	0.134	0.113	0.120

We have mainly found density data at atmospheric pressure in literature for comparison. For aqueous solutions of MDEA, Rinker et al. [19] measured the same compositions at T = (333.15 to 373.15) K, with the average absolute deviation between our data and the twelve points compared being 0.46 kg·m^{-3}. This value is consistent with the uncertainty of our measurements as occurs with other authors [20-25], the relative absolute deviations ranging from 0.02% to 0.08%. Zúñiga-Moreno et al. [26] published density data for this mixture up to 20 MPa, the deviations for the composition w_1 = 0.3 are consistent with the uncertainty but this is not true for w_1 = 0.2; it could be attributed to a slight difference in the composition. The relative deviations are shown graphically in Figure 3.

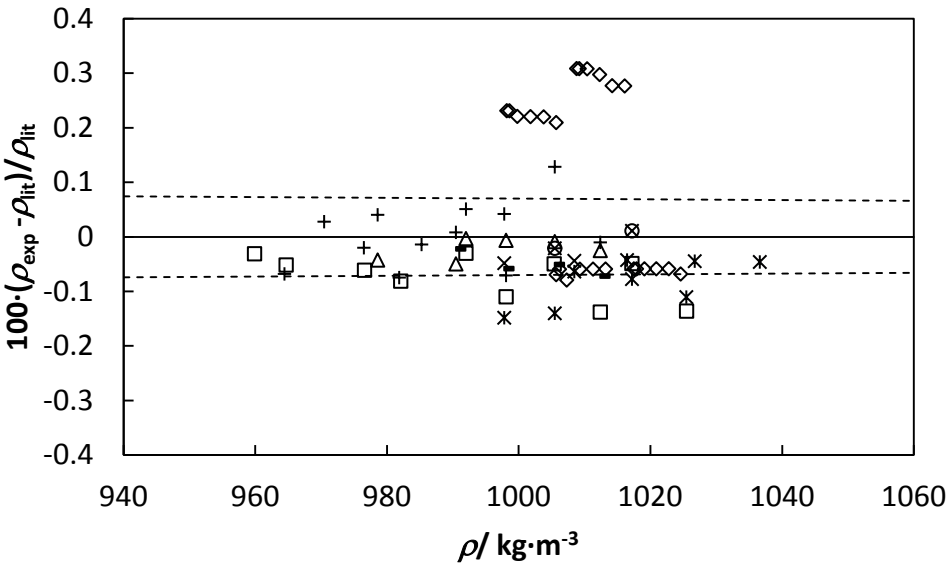

Figure 3. Relative deviation (%) of the experimental data of MDEA + H_2O density from the literature as a function of density: + Rinker et al. [19]; * Al-Ghawas et al. [20]; ○ Li et al. [21]; × Li et al. [22]; Δ Bernal-García et al. [23]; □ Han et al. [24]; – Pouryousefi et al. [25] and ◊ Zúñiga-Moreno et al. [26]. Dotted lines represent the relative expanded uncertainty of our measurements.

As regards MEA solutions, the relative absolute deviations, with different literature data, were 0.02% [25], with the same range of compositions and three temperatures at p = 0.1 MPa (twelve points in common), 0.14% [27] (only two points for comparison) 0.04% [28] (one point), 0.01% (four points in common) [29] and 0.06% [30] (ten points for comparison). Figure 4 shows these relative deviations.

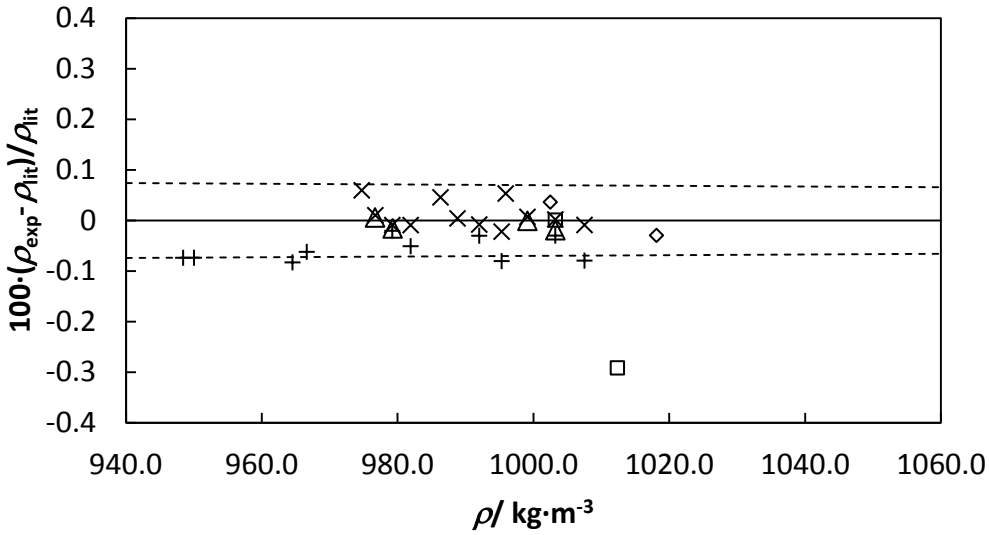

Figure 4. Relative deviation (%) of the experimental data of MEA + H_2O density from the literature as a function of density: × Pouryousefi et al. [25] ; □ Paul et al. [27]; ◊ Tseng et al. [28]; Δ Amundsen et al. [29] and + Han et al. [30]. Dotted lines represent the relative expanded uncertainty of our measurements.

Viscosity measurements of aqueous solutions of methyldiethanolamine (MDEA) and monoethanolamina (MEA) were performed for different amine mass fractions: 0.1, 0.2, 0.3 and 0.4, at p = (0.1 to 120) MPa and four temperatures from 293.15 to 353.15 K using the falling body viscometer. Experimental data are presented in table 8 for MDEA and table 9 for MEA.

It is important to remember the limits of the calibration used η = (0.630 to 4.929) mPa·s. This is why viscosities of 10% w MDEA + H_2O at T = 353.15 K, of 40% w MDEA + H_2O at T = 293.15 K, viscosities of 10% w MEA + H_2O at T = 353.15 K or of 20% w MEA + H_2O at T = 353.15 K (up to 40 MPa) are not given, since said viscosities were outside the calibration range and could not thus be measured using this calibration. However, there are certain viscosity values which are slightly below or above these limits imposed by calibration with *n*-dodecane which might be permissible considering their uncertainties.

Table 8. Experimental dynamic viscosities η, for the MDEA (1) + H_2O (2) system at different conditions of temperature, T, pressure, p, and mass fraction, w_1.[a]

T/K	p/MPa	w_1	η/mPa·s	w_1	η/mPa·s	w_1	η/mPa·s	w_1	η/mPa·s
293.15	0.1	0.1000	1.476	0.2002	2.350	0.3000	3.999		
293.15	5	0.1000	1.475	0.2002	2.353	0.3000	4.018		
293.15	10	0.1000	1.475	0.2002	2.357	0.3000	4.038		
293.15	20	0.1000	1.471	0.2002	2.364	0.3000	4.077		
293.15	30	0.1000	1.472	0.2002	2.372	0.3000	4.114		
293.15	40	0.1000	1.470	0.2002	2.380	0.3000	4.153		
293.15	60	0.1000	1.474	0.2002	2.399	0.3000	4.231		
293.15	80	0.1000	1.477	0.2002	2.419	0.3000	4.311		
293.15	100	0.1000	1.485	0.2002	2.437	0.3000	4.390		
293.15	120	0.1000	1.492	0.2002	2.464	0.3000	4.478		
313.15	0.1	0.1000	0.912	0.2002	1.345	0.3000	2.095	0.4000	3.238
313.15	5	0.1000	0.914	0.2002	1.347	0.3000	2.106	0.4000	3.270
313.15	10	0.1000	0.915	0.2002	1.349	0.3000	2.118	0.4000	3.302

313.15	20	0.1000	0.920	0.2002	1.358	0.3000	2.144	0.4000	3.365
313.15	30	0.1000	0.923	0.2002	1.367	0.3000	2.168	0.4000	3.428
313.15	40	0.1000	0.927	0.2002	1.377	0.3000	2.192	0.4000	3.491
313.15	60	0.1000	0.936	0.2002	1.398	0.3000	2.244	0.4000	3.618
313.15	80	0.1000	0.945	0.2002	1.418	0.3000	2.296	0.4000	3.740
313.15	100	0.1000	0.955	0.2002	1.445	0.3000	2.356	0.4000	3.866
313.15	120	0.1000	0.964	0.2002	1.466	0.3000	2.412	0.4000	3.996
333.15	0.1	0.1000	0.624	0.2002	0.872	0.3000	1.271	0.4000	1.843
333.15	5	0.1000	0.627	0.2002	0.876	0.3000	1.278	0.4000	1.861
333.15	10	0.1000	0.630	0.2002	0.881	0.3000	1.286	0.4000	1.880
333.15	20	0.1000	0.634	0.2002	0.890	0.3000	1.302	0.4000	1.921
333.15	30	0.1000	0.638	0.2002	0.898	0.3000	1.316	0.4000	1.956
333.15	40	0.1000	0.643	0.2002	0.907	0.3000	1.332	0.4000	1.992
333.15	60	0.1000	0.652	0.2002	0.924	0.3000	1.367	0.4000	2.063
333.15	80	0.1000	0.661	0.2002	0.942	0.3000	1.400	0.4000	2.134
333.15	100	0.1000	0.672	0.2002	0.967	0.3000	1.435	0.4000	2.206
333.15	120	0.1000	0.680	0.2002	0.982	0.3000	1.468	0.4000	2.280
353.15	0.1			0.2002	0.617	0.3000	0.854	0.4000	1.181
353.15	5			0.2002	0.620	0.3000	0.862	0.4000	1.193
353.15	10			0.2002	0.625	0.3000	0.869	0.4000	1.204
353.15	20			0.2002	0.633	0.3000	0.881	0.4000	1.229
353.15	30			0.2002	0.640	0.3000	0.894	0.4000	1.253
353.15	40			0.2002	0.647	0.3000	0.907	0.4000	1.276
353.15	60			0.2002	0.661	0.3000	0.932	0.4000	1.322
353.15	80			0.2002	0.675	0.3000	0.959	0.4000	1.368

353.15	100		0.2002	0.691	0.3000	0.997	0.4000	1.419
353.15	120		0.2002	0.705	0.3000	1.018	0.4000	1.467

[a] Standard uncertainties u are: $u(T) = 0.01$ K; $u_r(p) = 0.0001$ (kPa/kPa); $u(w) = 0.0001$; $u_r(\eta) = 0.015$ (mPa·s / mPa·s)

Table 9. Experimental dynamic viscosities η, for the MEA (1) + H_2O (2) system at different conditions of temperature, T, pressure, p, and mass fraction, w_1.[a]

T/K	p/MPa	w_1	η/mPa·s	w_1	η/mPa·s	w_1	η/mPa·s	w_1	η/mPa·s
293.15	0.1	0.1001	1.435	0.2000	1.968	0.3005	2.913	0.4001	4.315
293.15	5	0.1001	1.435	0.2000	1.970	0.3005	2.921	0.4001	4.340
293.15	10	0.1001	1.434	0.2000	1.969	0.3005	2.930	0.4001	4.368
293.15	20	0.1001	1.430	0.2000	1.973	0.3005	2.952	0.4001	4.426
293.15	30	0.1001	1.430	0.2000	1.977	0.3005	2.972	0.4001	4.475
293.15	40	0.1001	1.429	0.2000	1.983	0.3005	2.990	0.4001	4.528
293.15	60	0.1001	1.431	0.2000	1.994	0.3005	3.032	0.4001	4.628
293.15	80	0.1001	1.434	0.2000	2.009	0.3005	3.076	0.4001	4.739
293.15	100	0.1001	1.432	0.2000	2.026	0.3005	3.120	0.4001	4.845
293.15	120	0.1001	1.443	0.2000	2.046	0.3005	3.162	0.4001	4.954
313.15	0.1	0.1001	0.891	0.2000	1.173	0.3005	1.638	0.4001	2.284
313.15	5	0.1001	0.892	0.2000	1.178	0.3005	1.642	0.4001	2.306
313.15	10	0.1001	0.892	0.2000	1.182	0.3005	1.649	0.4001	2.319
313.15	20	0.1001	0.896	0.2000	1.190	0.3005	1.668	0.4001	2.352
313.15	30	0.1001	0.899	0.2000	1.197	0.3005	1.686	0.4001	2.384
313.15	40	0.1001	0.902	0.2000	1.205	0.3005	1.702	0.4001	2.416
313.15	60	0.1001	0.910	0.2000	1.219	0.3005	1.735	0.4001	2.479

313.15	80	0.1001	0.918	0.2000	1.232	0.3005	1.770	0.4001	2.544
313.15	100	0.1001	0.927	0.2000	1.249	0.3005	1.804	0.4001	2.609
313.15	120	0.1001	0.936	0.2000	1.263	0.3005	1.846	0.4001	2.675
333.15	0.1	0.1001	0.615	0.2000	0.780	0.3005	1.061	0.4001	1.389
333.15	5	0.1001	0.614	0.2000	0.788	0.3005	1.067	0.4001	1.401
333.15	10	0.1001	0.617	0.2000	0.792	0.3005	1.075	0.4001	1.410
333.15	20	0.1001	0.622	0.2000	0.799	0.3005	1.089	0.4001	1.434
333.15	30	0.1001	0.625	0.2000	0.807	0.3005	1.103	0.4001	1.453
333.15	40	0.1001	0.630	0.2000	0.815	0.3005	1.115	0.4001	1.475
333.15	60	0.1001	0.639	0.2000	0.829	0.3005	1.140	0.4001	1.518
333.15	80	0.1001	0.646	0.2000	0.844	0.3005	1.165	0.4001	1.559
333.15	100	0.1001	0.655	0.2000	0.859	0.3005	1.189	0.4001	1.600
333.15	120	0.1001	0.663	0.2000	0.874	0.3005	1.211	0.4001	1.645
353.15	0.1	0.1001		0.2000		0.3005	0.746	0.4001	0.942
353.15	5	0.1001		0.2000		0.3005	0.748	0.4001	0.944
353.15	10	0.1001		0.2000		0.3005	0.755	0.4001	0.957
353.15	20	0.1001		0.2000		0.3005	0.768	0.4001	0.975
353.15	30	0.1001		0.2000		0.3005	0.777	0.4001	0.989
353.15	40	0.1001		0.2000		0.3005	0.787	0.4001	1.006
353.15	60	0.1001		0.2000	0.607	0.3005	0.807	0.4001	1.039
353.15	80	0.1001		0.2000	0.619	0.3005	0.828	0.4001	1.068
353.15	100	0.1001		0.2000	0.632	0.3005	0.847	0.4001	1.097
353.15	120	0.1001		0.2000	0.644	0.3005	0.861	0.4001	1.128

[a] Standard uncertainties u are: $u(T) = 0.01$ K; $u_r(p) = 0.0001$ (kPa/kPa); $u(w) = 0.0001$; $u_r(\eta) = 0.015$ (mPa·s / mPa·s)

Viscosities of aqueous solutions of MDEA are always higher than viscosities of aqueous solutions of MEA under the same conditions of temperature, pressure and composition, as was also observed for densities. Viscosities of these mixtures increase at greater amine weight fractions and this effect is slightly higher for solutions with MDEA. Viscosity increases when pressure increases or temperature decreases, although the effect of temperature is much greater. These effects are similar for both amine solutions. Moreover, the increase in viscosity for higher amine weight fractions is more significant at lower temperatures.

Experimental viscosities were correlated using a modified VFT equation proposed by Comuñas et al. [31]:

$$\eta(T, p) = A\exp\left[\frac{B}{T-C}\right]\exp\left[D\ln\left(\frac{p+E(T)}{0.1+E(T)}\right)\right] \quad (4)$$

where

$$E(T) = E_0 + E_1 T + E_2 T^2 \quad (5)$$

The results of the correlation, which include the fitting parameters and the standard deviations, are summarized in table 10. The standard deviations obtained from the fittings are lower than the uncertainties of the experimental measurements and thus the correlation model is suitable for describing the viscosity behaviour of this kind of mixtures.

Table 10. Fitting parameters of equation (4) and standard deviation for the viscosity measurements.

MDEA (1) + H_2O (2)	w_1 = 0.1	w_1 = 0.2	w_1 = 0.3	w_1 = 0.4
A/mPa·s	0.0015	0.0014	0.0013	0.0018
B/K	1901.9	1903.5	1904.9	1905.1
C/K	17.572	37.900	57.019	59.773
D	1.0238	1.3329	4.9634	0.9208

E_0/MPa	2.3741	1.4751	1.4549	-0.1803
E_1 /MPa·K^{-1}	214.85	76.776	72.212	3.5386
E_2 /MPa·K^{-2}	-0.6354	-0.2212	-0.1853	-0.0065
σ/mPa·s	0.0080	0.0122	0.0213	0.0190
MEA (1) + H_2O (2)	w_1 = 0.1	w_1 = 0.2	w_1 = 0.3	w_1 = 0.4
A/mPa·s	0.0015	0.0015	0.0015	0.0014
B/K	1901.8	1902.7	1903.7	1904.8
C/K	15.502	27.922	40.915	55.404
D	0.9940	0.9488	3.0065	0.8551
E_0/MPa	3.0884	1.4267	1.4864	-0.7075
E_1 /MPa·K^{-1}	326.09	69.048	79.220	8.8161
E_2 /MPa·K^{-2}	-0.9687	-0.2005	-0.2188	-0.0220
σ/mPa·s	0.0078	0.0086	0.0205	0.0219

In order to check the reliability of viscosity data, a comparison was carried out at atmospheric pressure (due to the lack of these values at high pressures) between viscosities obtained with our falling body viscometer and the ones obtained using a Stabinger SVM 3000 viscometer available in our laboratory (table 11).

Table 11. Viscosity comparison between falling body viscometer (FB)[a] at p = 0.1 MPa and Stabinger SVM 3000 viscometer (SVM)[b] at p = 0.093 MPa (atmospheric pressure) for the mixtures studied.

		MDEA (1) + H_2O (2)			MEA (1) + H_2O (2)		
w_1	T/K	η_{FB}/mPa·s	η_{SVM}/mPa·s	% deviation	η_{FB}/mPa·s	η_{SVM}/mPa·s	% deviation
0.1	293.15	1.476	1.463	0.9	1.435	1.409	1.8
0.1	313.15	0.912	0.9079	0.4	0.891	0.8932	-0.3

0.1	333.15	0.624	0.6344	-1.6	0.615	0.6263	-1.8
0.2	293.15	2.350	2.293	2.4	1.968	1.982	-0.7
0.2	313.15	1.345	1.342	0.2	1.173	1.198	-2.2
0.2	333.15	0.872	0.8719	0.0	0.780	0.7832	-0.4
0.2	353.15	0.617	0.6205	-0.6			
0.3	293.15	3.999	3.942	1.4	2.913	2.967	-1.9
0.3	313.15	2.095	2.094	0.0	1.638	1.675	-2.2
0.3	333.15	1.271	1.276	-0.4	1.061	1.084	-2.1
0.3	353.15	0.854	0.8505	0.4	0.746	0.7640	-2.4
0.4	293.15				4.315	4.326	-0.3
0.4	313.15	3.238	3.145	2.9	2.284	2.284	0.0
0.4	333.15	1.843	1.820	1.2	1.389	1.405	-1.2
0.4	353.15	1.181	1.186	-0.4	0.942	0.9518	-1.0

[a] Standard uncertainties u are: $u(T) = 0.01$ K; $u_r(p) = 0.0001$ (kPa/kPa); $u(w) = 0.0001$; $u_r(\eta) = 0.015$ (mPa·s / mPa·s)

[b] Standard uncertainties u are: $u(T) = 0.02$ K; $u_r(p) = 0.\ 005$ (kPa/kPa); $u(w) = 0.0001$; $u_r(\eta) = 0.005$ (mPa·s / mPa·s)

As regards the compatibility of the results obtained using the falling body viscometer and the Stabinger viscometer, the maximum deviation is 2.9 % which corresponds to the mixture 40 % w MDEA at T = 313.15 K (3.2382 mPa·s given by FB vs 3.1448 mPa·s given by SVM). This deviation is acceptable in light of the uncertainty values given for the falling body equipment combined with the expanded uncertainty of ± 1 % for SVM 3000.

After checking the compatibility of both viscometers, the values obtained with the falling body equipment will also be compared with literature values [19,20,22,23,27,32-35], at atmospheric pressure. A summary of the literature used in figure 5 is given in table 12.

Table 12. Literature data used to compare of the experimental viscosities measured in this work.

Literature	systems	conditions
Rinker et al. [19]	MDEA (1) + H_2O (2)	w_1 = 0.1 T = 333.15 K w_1 = 0.2; 0.3; 0.4 T = (333.15-353.15) K
Al-Ghawas et al. [20]	MDEA (1) + H_2O (2)	w_1 = 0.1; 0.2; 0.3 T = (293.15-333.15) K w_1 = 0.4 T = 313.15 K
Li et al. [22]	MDEA (1) + H_2O (2)	w_1 = 0.2; 0.3 T = (313.15-333.15) K w_1 = 0.4 T = 313.15 K
	MEA (1) + H_2O (2)	w_1 = 0.2; 0.3 T = (313.15-333.15) K
Paul et al. [27]	MDEA (1) + H_2O (2)	w_1 = 0.1; 0.2; 0.3 T = (313.15-333.15) K
Arachchige et al. [32]	MDEA (1) + H_2O (2) MEA (1) + H_2O (2)	w_1 = 0.1; 0.2 T = (293.15-333.15) K w_1 = 0.3; 0.4 T = (293.15-353.15) K
Teng et al. [33]	MDEA (1) + H_2O (2)	w_1 = 0.1; 0.2; 0.3; 0.4 T = (313.15-353.15) K
Bernal-García et al. [34]	MDEA (1) + H_2O (2)	w_1 = 0.3; 0.4 T = (313.15-353.15) K
Maham et al. [35]	MEA (1) + H_2O (2)	w_1 = 0.1; 0.2; 0.3; 0.4 T = (313.15-333.15) K w_1 = 0.3; 0.4 T = 353.15 K

Percentage deviations from those reference values are plotted in figure 5 as a function of viscosity. Uncertainties, which are represented by the two converging lines, are considered to vary linearly between the values ± 2.4 % and ± 2.9 % shown before.

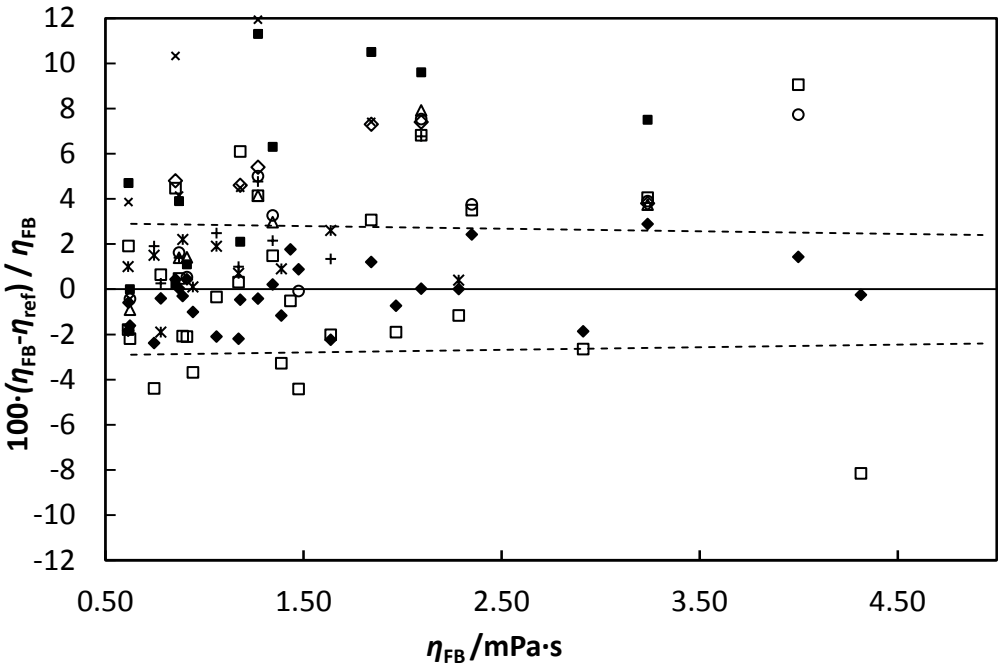

Figure 5. Relative deviation (%) of the experimental data of MDEA + H_2O and MEA + H_2O dynamic viscosity from the literature as a function of viscosity: ♦ Stabinger SVM 3000; × Rinker et al. [19]; ○ Al-Ghawas et al. [20]; + Li et al. [22]; Δ Paul et al. [27]; □ Aranchchige et al. [32]; ■ Teng et al. [33]; ◊ Bernal-García et al. [34] and * Maham et al. [35]. Lines represent the relative expanded uncertainty of our measurements.

Figure 5 shows a certain scattering among all data, which might be justified due to the intrinsic difficulty of measuring viscosity. In this sense, it is not possible to analyze quantitatively the compatibility of our data with others from the literature because most of literature values do not provide their associated uncertainties according to JCGM guide. However, knowing the uncertainties of both the falling body and the Stabinger SVM 3000 viscometers has made it possible to evidence the compatibility of their results. For MEA

solutions, the best results were obtained in comparison with Maham et al. [30] with an average relative deviation of 1.3% (ten points for comparison) and these values were 3.4% in comparison with Al-Ghawas et al. [20] (ten points for comparison) and 3.8% with Aranchchige et al. [32] (fourteen points), for MDEA solutions.

5. Conclusions

Viscosity and density measurements of MDEA + H_2O and MEA + H_2O mixtures (10%, 20%, 30% and 40% amine mass fraction), at wide pressure and temperature ranges are presented. A recently developed falling body viscometer, able to measure viscosities of liquids from 0.1 MPa to 140 MPa and from 253.15 K to 523.15 K, is used in this work. It has been calibrated with *n*-dodecane and 1-butanol in a temperature range from 293.15 K to 353.15 K and pressures up to 120 MPa, obtaining a calibration range η = (0.630 to 4.929) mPa·s. A detailed study of uncertainties was carried out, obtaining relative expanded uncertainties (k = 2) between ± 2.4% (4.954 mPa·s) and ± 2.9% (0.617 mPa·s).

In order to obtain said viscosities, densities were needed. These were obtained with an Anton Paar DMA HPM densimeter with an associated expanded uncertainty (k = 2) of ± 0.7 kg/m^3.

Density and viscosity measurements were fitted using modified Tamman-Tait and VFT equations, respectively, obtaining standard deviations better than uncertainty measurements.

Finally, the agreement of viscosity results of the falling body viscometer and Stabinger SVM 3000 at atmospheric pressure has been shown, and is completed with an exhaustive comparison to literature data. Both properties for MDEA solutions are always higher than for of MEA solutions under the same conditions. They decrease significantly when temperature increases and increase with pressure. Changes with temperature and pressure are quite similar for both amines although changes due to amine composition are more relevant for MDEA solutions.

Acknowledgments

The authors M.S. and E.I.C. thanks to Education Ministry (Spanish Government) through a FPU scholarship and to Project for European Latin American Cooperation and Exchange (PEACE), respectively, for doctoral studies. The work was funded by the Regional Government of Castilla y León through the Project VA295U14.

References

[1] G.F. Versteeg, W.P.M. Van Swaaij, Chem. Eng. Sci. 43 (1988) 587–591.

[2] R.J. Little, W.P.M. Van Swaaij, G.F. Versteeg, AIChE J. 36 (1990) 1633-1640.

[3] A. Veawab, A. Aroonwilas, P. Tintiwachwuthikul, ACS Division of Fuel Chemistry Preprints 47 (2002) 49-50.

[4] D. Aaron, C. Tsouris, Separation Sci. & Tech. 40 (2005) 321-348.

[5] C. Hsu, M. Li, J. Chem. Eng. Data 42 (1997) 502–507.

[6] J.J. Segovia, O. Fandiño, E.R. López, L. Lugo, M.C. Martín, J. Fernández, J. Chem. Thermodyn. 41 (2009) 632–638.

[7] J.R. Zambrano, M. Sobrino, M.C. Martín, M.A. Villamañán, C.R. Chamorro, J.J. Segovia, J. Chem. Thermodyn. 96 (2016) 104-116.

[8] Evaluation of measurement data - Guide to the expression of uncertainty in measurement. JCGM 2008.

[9] P. Daugé, A. Baylaucq, L. Marlin, C. Boned, J. Chem. Eng. Data 46 (2001) 823-830.

[10] W.A. Wakeham, A. Nagashima, J.V. Sengers, Experimental Thermodynamics, Vol. III: Measurement of the Transport Properties of Fluids, Blackwell Scientific Publications, Oxford, 1991.

[11] M. Zeng, C.J. Schaschke, Int. J. Chem. Eng. (2009) 1-8.

[12] M.J.P. Comuñas, X. Paredes, F.M. Gaciño, J. Fernández, J.P. Bazile, C. Boned, J.L. Daridon, G. Galliero, J. Pauly, K.R. Harris, J. Chem. Thermodyn. 69 (2014) 201-208.

[13] J.R. Zambrano, M. Sobrino, M.C. Martín, M.A. Villamañán, C.R. Chamorro, J.J. Segovia, J. Chem. Thermodyn. (2016) http://dx.doi.org/10.1016/j.jct.2015.12.021.

[14] M. Sobrino, J.J. Segovia, Dyna 87 (2012) 438-445.

[15] M.C.S. Chen, J.A. Lescarboura, G.W. Swift, AIChE J. 14 (1968) 123-127.

[16] C.J. Schaschke, S. Allio, E. Holmberg, Food Bioprod. Process. 84 (2006) 173-178.

[17] M. Sobrino, Desarrollo de un viscosímetro para la caracterización a alta presión de nuevos biocombustibles y mezclas acuosas de aminas para la captura de CO_2, PhD Thesis, University of Valladolid, Spain, 2015.

[18] D.R. Caudwell, J.P. Trusler, V. Vesovic, W.A. Wakeham, International Journal of Thermophysics 25 (2004) 1339-1352.

[19] E.B. Rinker, D.W. Oelschlager, A.T. Colussi, K.R. Henry, O.C. Sandall, J. Chem. Eng. Data 39 (1994) 392–395.

[20] H.A. Al-Ghawas, D.P. Hagewlesche, G. Ruiz-Ibanez, O.C. Sandall, J. Chem. Eng. Data 34 (1989) 385–391.

[21] M. Li, K. Shen, J. Chem. Eng. Data 37 (1992) 288-290.

[22] M. Li, Y. Lie, J. Chem. Eng. Data 39 (1994) 444-447.

[23] J.M. Bernal-García, M. Ramos-Estrada, G.A. Iglesias-Silva, K.R. Hall, J. Chem. Eng. Data 48 (2003) 1442-1445.

[24] J. Han, J. Jing, D.A. Eimer, M.C. Melaaen, J. Chem. Eng. Data 57 (2012) 1843-1850.

[25] F. Pouryousefi, R.O. Idem, Ind. Eng. Chem. Res. 47 (2008) 1268-1276.

[26] A. Zúñiga-Moreno, L.A. Galicia-Luna, J.M. Bernal-García, G.A. Iglesias-Silva, J. Chem. Eng. Data 52 (2007) 1988-1995.

[27] S. Paul, B. Mandal, J. Chem. Eng. Data 51 (2006) 1808–1810.

[28] Y.M. Tseng, R. Thompson J. Chem. Eng. Data 9 (1964) 264-267.

[29] T.G. Amundsen, L.E. Øi, D.A. Eimer J. Chem. Eng. Data 54 (2009) 3096–3100.

[30] J. Han, J. Jing, D.A. Eimer, M.C. Melaaen, J. Chem. Eng. Data 57 (2012) 1095-1103.

[31] M.J.P.Comuñas, A. Baylaucq, C. Boned, J. Fernández, Int. J. Thermophys. 22 (2001) 749-768.

[32] U.S.P.R. Arachchige, N. Aryal, D.A. Eimer, M.C. Melaaen, Annual Transact. Nordic Rheology Soc. 21 (2013) 299–306.

[33] T.T. Tseng, Y. Maham, L.G. Hepler, A.E. Mather, J. Chem. Eng. Data 39 (1994) 290-293.

[34] J.M. Bernal-García, L.A. Galicia-Luna, K.R. Hall, M. Ramos-Estrada, G.A. Iglesias-Silva, J. Chem. Eng. Data 49 (2004) 864-866.

[35] Y. Maham, C.N. Liew, A.E. Mather, J. Sol. Chem. 31 (2002) 743-756.